Integration of AVO Analysis and Seismic Inversion for Reservoir Characterization of an Oil Field, Niger Delta, Nigeria

.

ABSTRACT

This study analyses the characteristics of the G-field reservoirs using Amplitude-Versus-Offset (AVO) analysis and seismic inversion. Well log data were obtained from four deviated wells G-14, G-15, G-16, and G-17, and delineated using a combination of gamma and resistivity logs. The suitable well logs analyzed were interpreted and used for the modeling of AVO and its analysis. Post-stacked 3D seismic data volume that covers an area of 266.68 km^2 was also utilized, within which the four available wells are situated. Well correlation and seismic-to-well tie was done to facilitate horizon mapping on the seismic data and the data set was then inverted into an impedance volume using model-based and neural network inversion. AVO analysis results using G–14 show a small negative intercept with subsequently higher amplitudes as the offset increases demonstrating a Class II. The data slices of the extracted acoustic impedance, Mu–Rho, and Lambda–Rho volumes for the model-based inversion shows low values for hydrocarbon reservoir sand, especially around the producing wells, and high values for non reservoir sand for both acoustic impedance and Lambda–Rho which is consistent with fluid determination while it was medium to high values around well locations indicating hydrocarbon bearing sand for both Mu–Rho and shear impedance. For the neutral network inversion method, the data slices of V_P/V_S, water saturation, and porosity shows that the four wells are located in areas with low V_P/V_S and water saturation with very high porosity values indicating the presence of hydrocarbon.

Keywords: AVO, inversion, model-based, neural network

1. INTRODUCTION

Techniques on reservoir characterization using seismic amplitudes have been published over the years, including works on seismic attribute analysis and amplitude variations with offset (AVO). Bright spots also known as large reflection amplitudes were acknowledged in the early 1970s as potential hydrocarbon indicators [1, 2].

Reservoir characterization refers to all the relevant data that is essential to describing a reservoir's ability to produce and store hydrocarbons [3]. This entails understanding the reservoir's overall architecture, the fluid flow within the reservoir, as well as its internal and external geometry, and its model with the reservoir properties distribution [3]. Such information aids in the prediction of future reservoir performance, rejuvenation of oil fields, the production rates improvement, and reduction of cost expenditure, and helps to develop accurate financial models for oil companies management. Considered a crucial phase between the discovery of oil and gas fields and the reservoir management phase, to compile all the above-mentioned information, it integrates the technical disciplines of reservoir engineering economics and data management geophysics, geology, and petro-physics [3].

The success of the reservoir characterization is determined by how well the above disciplines are integrated, a subtle goal in some cases, with the success of each varying project [4].

Seismic inversion is the extraction of the underlying geology from seismic data [5]. For this to be achieved, impedance, which is an interval attribute for estimating properties such as porosity, is derived from seismic data. Geoscientists have used this method as a critical tool in depleting the risks associated with oil and gas exploration, development, and production. Its primary applications are in petro-physical studies and reservoir characterization because layer information is extended around the seismic volume at well locations, leading to true subsurface geology delineation. It is also used in converting a noisy, seismic trace into sonic and density logs. The inverse of transforming these two logs into a synthetic [6] helps remove anomalies of wavelets and then estimates a better resolution for reservoir properties. The goal of seismic inversion is executed with the aim of determining the contrasts between rock properties such as compressional-wave velocities, shear wave velocities, and densities. The observed variation of the amplitudes of the reflected waves with the angle of incidence can be used to evaluate these contrasts. It is vital to construct the inputs for the inversion workflow in an optimized manner in order to perform seismic inversion [7].

“The AVO (amplitude variation with offset) technique evaluates changes in seismic reflection amplitude with alterations in distance between shot points and receivers. With AVO analysis Geophysicists can evaluate reservoir rock properties such as lithology, fluid content, porosity, and density better with greater accuracy” [8]. AVO analysis today is commonly used in lithology identification, hydrocarbon detection, and fluid parameter analysis because variations in physical properties just above and below the boundaries affect seismic amplitudes. A growing number of theories and techniques in seismic data processing, interpretation, and acquisition have been employed, updated, and developed in recent years making AVO analysis in theory and practice increasingly fascinating.

Seismic impedance inversion in addition to AVO is another technique for lithofacies identification. Due to a study that found gas-sand-capped shale to have an amplitude variation with offset in pre-stack seismic data [9], AVO became a commercial tool for hydrocarbon prediction [10, 11]. In many regions, amplitude variation with offset (AVO) analysis has been widely used to predict fluid and lithology [9, 12]. All offset-dependent amplitude effects, except the reflection coefficient, are assumed to be corrected in traditional AVO inversion. Aside, from the lithology identification, another effective area of research centers on the application of amplitude information in tomographic inversion to ascertain elastic properties and subsurface structure [13, 14]

For direct hydrocarbon identification (DHI), [15] employed Amplitude versus Angle (AVA) techniques and Pre-Stack seismic inversion to better comprehend and reduce the risk of hydrocarbon prospecting. A wedge model’s inverted seismic response and its correlation with real seismic proved useful for detecting hydrocarbons in saturated zones. As a result, AVA effects on angle gathers provided basic information on the lithology and pore fill contents of the rocks being studied. AVA modeling, together with fluid substitution and rock physics, increased the comprehension of the observed seismic response and provided a sophisticated tool for hydrocarbon prospect de-risking [15].

Rock physics with impedance techniques and AVO reflectivity was employed by [16] as an integrated method to delineate and characterize lithology and fluid effects, as well as map the seismic signature in a soft sandstone reservoir in offshore Niger Delta and it was concluded that P-impedance, Poisson's ratio, and rock physics relations are highly effective

in discriminating gas sands and their generated cross-plots points clusters separated from the background trend. Furthermore, the integration of rock physics principles to reduce seismic ambiguities/complexities has become an important technique in quantitative seismic interpretation in recent past decades [17, 18,19].

Reservoir characterization was carried out for hydrocarbon detection using Amplitude Variation with Angles constrained by localized rock physics template on a poorly compacted sandstone reservoir of the 'Jay' Field [19]. "Different seismic amplitude reflections from the field reservoirs were investigated to determine the effect of fluids and lithologies on the observed seismic amplitudes for possible hydrocarbon identification away from the well location. Amplitude variation with angles (AVA) and rock physics techniques was used to analyze amplitude responses from sandstone reservoirs and was extracted from the near and far partial angle stacks to identify changes in amplitudes with angles" [19]. "Thereafter, Rock Property Template (RPT) analyses were used to determine the influence of the reservoir properties on seismic responses. The good logs result revealed that three of the seven identified reservoirs (Sands A, B, and C) were brine saturated, Sand D is oil while Sands E, F, and G are gas bearing [19]. The result of the changes in seismic amplitudes from near to far angles around the Well location shows that the gas reservoirs produce different AVOs that correspond to Classes II, III, and IV respectively, and the established well log RPT supports AVA results of gas presence in the identified area away from the well location. This helps to reduce the risk associated with seismic amplitude ambiguities and enhanced the certainty of gas present at the location away from the good log information" [19].

Previous work [20] investigated the unrelated seismic amplitude responses detected in sandstone reservoirs with the same fluid saturation in their article "Reservoir Fluid Determination from Angle Stacked Seismic Volumes in 'Jay' Field, Niger Delta, Nigeria.". Their report aided in demonstrating the perceptive implications of the distinctive amplitudes reflected from hydrocarbon reservoirs and identified probable gas accumulation locations in the 'Jay' Field using angle-stacked seismic volume. They concluded that the integration of Lambda Mu-Rho, AVA, and Elastic impedance inversions aids the detection of the presence of gas in the identified area away from the well location [20]. Within the "XY" field offshore the Niger Delta, [21] used AVO inversion to delineate the presence of gas reservoirs within the field of study. They reported that while the inverted results and cross-plots of good data were able to delineate the gas reservoirs, the AVO inversion analysis method was a better seismic interpreter to understand the physical properties of the zone of interest; as the conventional AVO inversion analysis was unable to distinguish the gas reservoirs because there are other zones with similar signatures [21].

"The integration of AVO reflectivity and rock physics was used to characterize lithologies and fluid effects in soft sandstone reservoir, deep water offshore block of the Agbada Formation, Niger Delta Basin" [16, 19]. "The study revealed Class IV AVO gas sand in the deep-water block to support the effectiveness of integrating relevant methods for soft gas sand discrimination in the deep offshore field. The amplitude variation with offset signatures and seismic fluid sensitivities at a determined depth of burial was predicted by the combination of the burial history and rock-physics modeling of sand and shale" [19, 22]. AVO attributes were applied in facies and hydrocarbon prediction [19, 23] and also to discriminate between different seismic responses [19, 24]. [25] established an important relationship between reservoir parameters such as porosity and clay content and seismic responses [19]. Meanwhile, [26] used Biot-Gassmann fluid substitution, AVO, and cross plot model techniques to evaluate the physics of reservoir rocks by investigating the sensitivity of some basic rock properties for hydrocarbon exploration in the Niger Delta field and the study

showed that the reservoir sand produced Class IV AVO response and 5% gas presence in the reservoir resulted to the significant change in the rock properties [19].

This study is aimed at evaluating the reservoir characteristics through seismic AVO analysis and inversion by examining and delineating hydrocarbon-bearing reservoirs and Integrating AVO analysis and seismic inversion for reservoir characterization.

1.1 Location of the Study Area

The study area is an oil field is located within the onshore, south-western part of the coastal swamp depobelt region of the Niger Delta, within latitude 3°N and 6°N and longitude 5°E and 8°E (Fig. 1).

Fig.1. Location of the study area (G–field highlighted by the blue hashed square) [27].

1.2 Geology of the Study Area

The onshore portion of the Niger Delta Province is characterized by the geology of southwestern Cameroon and southern Nigeria, which is bounded in the north by the Benin flank-an east-northeast trending hinge line that extends south of the West Africa Basement massif [28]. The Cretaceous on the Abakiliki High is defined to the north-east by outcrops and to the east-south-east by the Calabar flank-a hinge line bordering the adjacent Precambrian basement (Fig. 2), extending from longitudes 3°E–9°E and latitudes 4° 30′ N–5° 20′ N [28, 29]. The Niger Delta, situated in the Gulf of Guinea of West Africa and extends throughout the Niger Delta Province, contains the Tertiary Niger Delta Petroleum System [28, 29, 30].

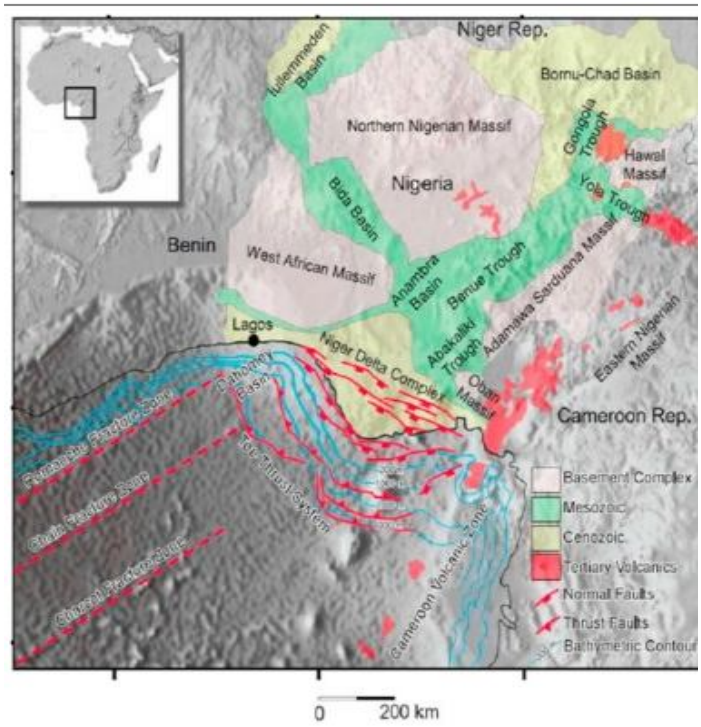

Fig. 2. Niger Delta map showing the main sedimentary basins and tectonic features [31].

According to [29] from the Eocene to the present, the delta has formed depobelts that represent the most active portion at each development stage pro-grading south-westward [32]. With an area of about 300,000 km^2 [33], a sediment thickness of over 10 km in the basin depo-center [34], and sediment volume of 500,000 km^3 [35] these deposits form one of the largest regressive deltas in the world [33].

The Niger Delta basin is subdivided into Paralic Agbada, the Marine Akata shale, and continental Benin sand (freshwater). Hydrocarbon reservoirs are most commonly found in the Agbada formation where the in situ connate brine has been superseded by the hydrocarbons [29]. This hydrocarbon zone is made up of thousands of individual reservoirs, the majority of which are sandstone pockets, trapped within oil-rich shale strata [29]. The reservoir rocks are sand intercalations, while the hydrocarbon source rocks are organic matter-rich shale [29]. The lithologic identification in the Agbada formation of the Niger Delta is primarily shale or sand, and as such, suggests that AVO analysis would be better suited to predicting the fluid type in reservoirs [29].

1.3 Amplitude versus offset (AVO)

The AVO (amplitude variation with offset) technique evaluates changes in seismic reflection amplitude with alterations in distance between shot points and receivers. Geophysicists use AVO analysis to better evaluate reservoir rock properties such as lithology, fluid content, porosity, and density [36]. AVO theory uses the reflection amplitudes of seismic gathers to explain the relationship between the rock's elastic properties and the prediction of the pore fluid effect. The theory was developed based on the splitting by adjacent elastic media of dissimilar elastic properties at boundaries caused by seismic energy segregation. When a seismic wave strikes a boundary part, energy is converted to reflected and transmitted energy. The amplitudes of the reflected and transmitted energy are determined by the

physical properties across the boundary and the difference in the incidence angle of the original ray [37]. The major elastic or physical properties here are the compressional wave velocity (Vp), shear wave velocity (Vs), and density (ρ). The impact of rock pore fluids and petro-physical properties on these elastic parameters makes AVO analysis an effective tool in delineating lithology and pore fluid types [38].

Rutherford and Williams's classification of the reflection coefficient curves has become the industry standard and it is associated respectively with bright spot, phase reversal, and dim out classified in the1970s [39]. [39] proposed the first AVO classification for gas sands based on the normal incidence P-wave reflection coefficient, which was expanded by [11]. Fig. 3 shows the general classification with the addition of a "flat spot" curve, representing typical hydrocarbon-water contacts.

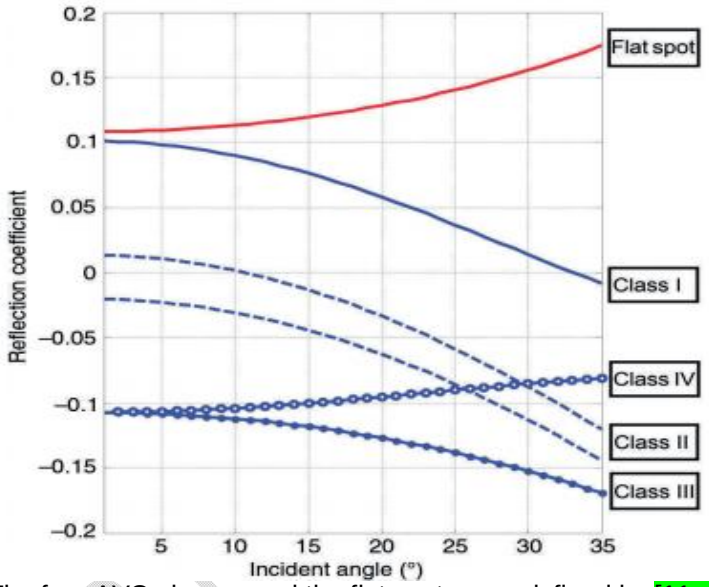

Fig. 3. The four AVO classes and the flat spot curve defined by [11, 39]

The classification was developed for reflections from hydrocarbon-saturated formations. According to Rutherford and Williams's classification, the slope of the reflection coefficient curve is negative for all classes [39]. The amplitude of reflection decreases with the incidence angle. When high-impedance sand lies beneath a lower-impedance shale layer, Class I reflections occur. The zero offset reflection coefficient (and thus the intercept) is positive; in general, the amplitude decreases with an increasing angle of incidence. However, the absolute amplitude can increase with the angle of incidence as depicted for Class II and III AVO gas-saturated anomalies. The impedance observed in Class II is quite small and very small positive reflection coefficients are usually noticed at the reservoir top, which then converts to a negative value at far offsets [11, 39]. This type is referred to as "Phase or Polarity Reversals". Class II is made of near-zero reservoirs. They can be described as both weak positive (Class IIp) or negative (Class II) intercept gradients. Because of the phase reversal inherent in this response, [40] proposed in 1995 that the small positive Class-II response be referred to as Class-IIp (Fig. 4).

In Class III, negative reflection is observed at the top of the reservoir. As the angle of incidence increases, the amplitudes become more negative. This is referred to as "Bright Spots". In this situation, polarity change does not occur. Class III reflections occur when low-impedance sand is underlined by higher-impedance shale. The zero offset reflection

coefficient is negative and the intercept and gradient are both strongly negative; the negative amplitudes increase in size with increasing angle of incidence [37]. Certain Class III gas-saturated anomalies can have slowly decreasing amplitudes with offset [11]. These were named Class IV AVO anomalies. However, the large amplitude associated with the hydrocarbons remains the primary diagnostic feature for Class IV anomalies.

Class 4 has a lower impedance with an amplitude that is declining against the offset and negative reflection coefficient at zero offsets, it is the only anomaly with a positive gradient. There is a polarity change at a certain angle and increasing amplitude proportionally to the offset [10].

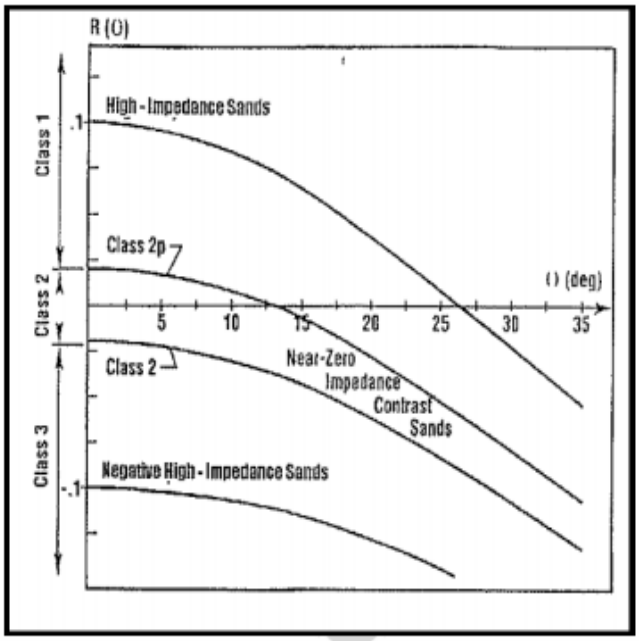

Fig. 4. Anomaly amplitude classification showing the two types of Class 2 AVO [10, 39]

2. MATERIALS AND METHODS

The data set for this work included a suite of well logs (containing well deviation and log data, well header and check shots) obtained from four deviated wells; G-14, G-15, G-16, and G-17. The composite logs are shown in Figs. 5 – 8. Table 1 shows the unit and symbols of the various logs, while the well header information is given in Table 2. Also, a 3D post-stack seismic data in SEG-Y format (processed seismic data) gathered from east-west located receivers with the angle of 90(0 at Crossline direction +90) containing 961 inlines and 444 crosslines covering an area of 266.67km^2, within which the 4 available wells are situated. Fig. 9 shows the base map of the seismic field. The data were acquired from G-Field located in the onshore Niger-Delta. Hampson Russell (HR) software suite was used for the data processing, well log data loading and cross-plot analysis, hence the well logs including log headers are in LAS formats. The inversion is also performed using Strata package from Hampson-Russell software.

The seismic data utilized in this study is a post stacked 3D seismic data volume acquired in the Niger Delta. The seismic data covers an area of approximately 266.68km^2, within which the 4 available wells are situated. Fig. 8 shows the base map of the seismic field. The data contains 961 inlines and 444 crosslines with 25ft spacing between each. The quality of the data is fair within the range of interest except its cut off 1999 on the Inline and 11990 on the Crossline.

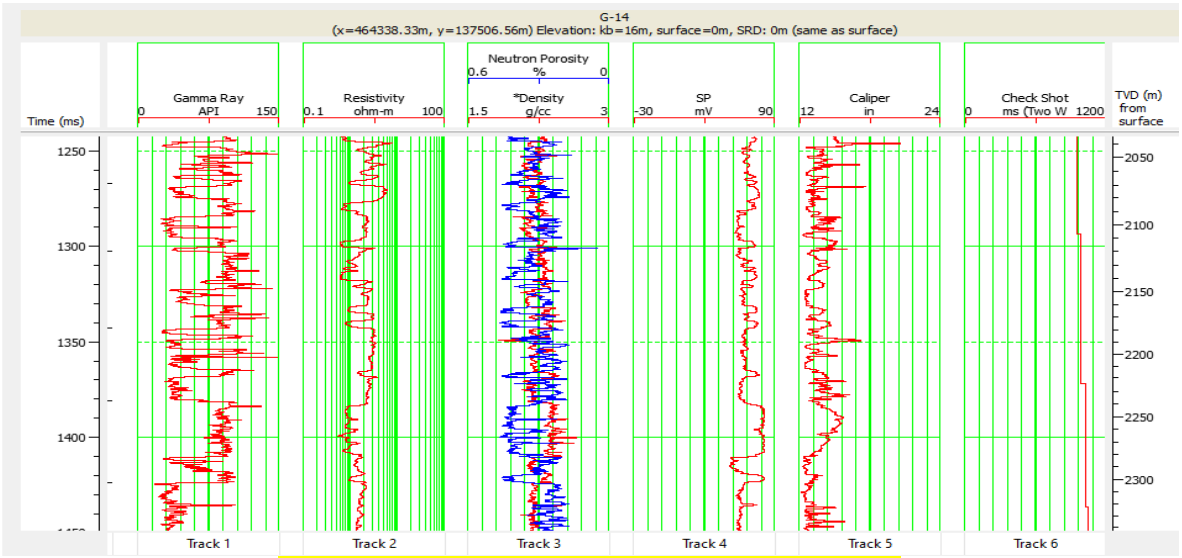

Fig. 5. Typical log section displays of raw log suite for G-14.

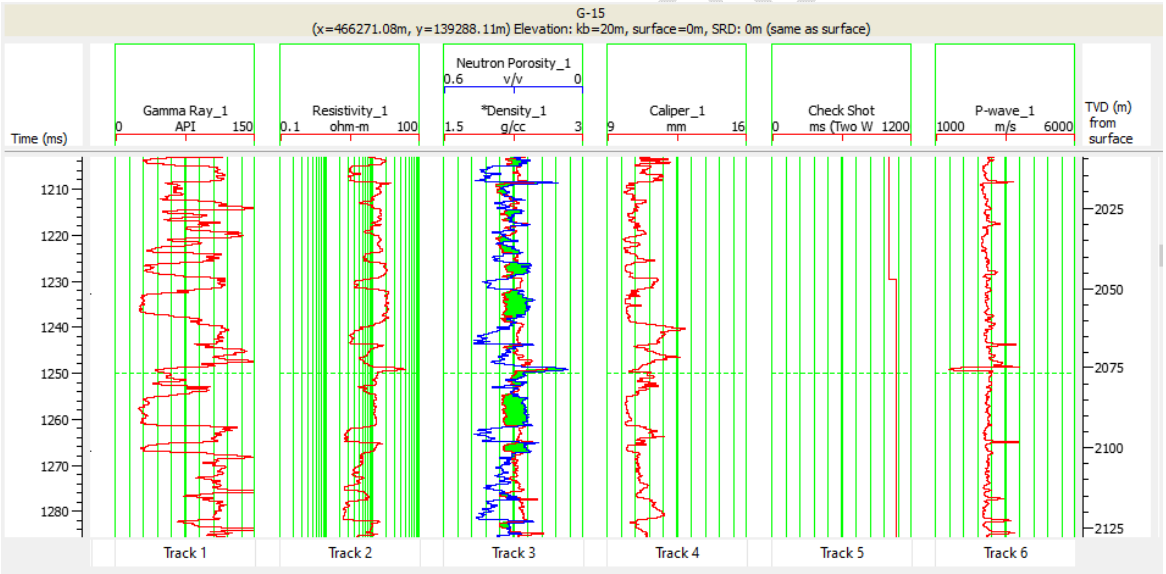

Fig. 6. Typical log section displays of raw log suite for G-15.

Table 1. Different types of logs included their acronyms and units of measure.

ACRONYM	UNITS	TYPES OF WELL
GR	API	Gamma Ray
SP	Mv	Spontaneous Potential
DT	µs/ft	Compressional Sonic
RHOB	g/c3	Bulk Density
CAL	Inches	Caliper
NPHI	v/v	Neutron porosity
CS	Ms	Checkshot
RT	Ohm-m	True Resistivity

Table 2. Seismic data header information for the Wells,

WELL NAME	UNIT	X-LOCATION	Y-LOCATION	INLINE	XLINE	CDP
G-14	M	464338.33	137506.56	11498	1864	114660
G-15	M	466271.08	139288.11	11575	1935	148919
G-16	M	466266.32	139283.72	11575	1935	148919
G-17	M	468376.88	140677.54	11660	1991	186715

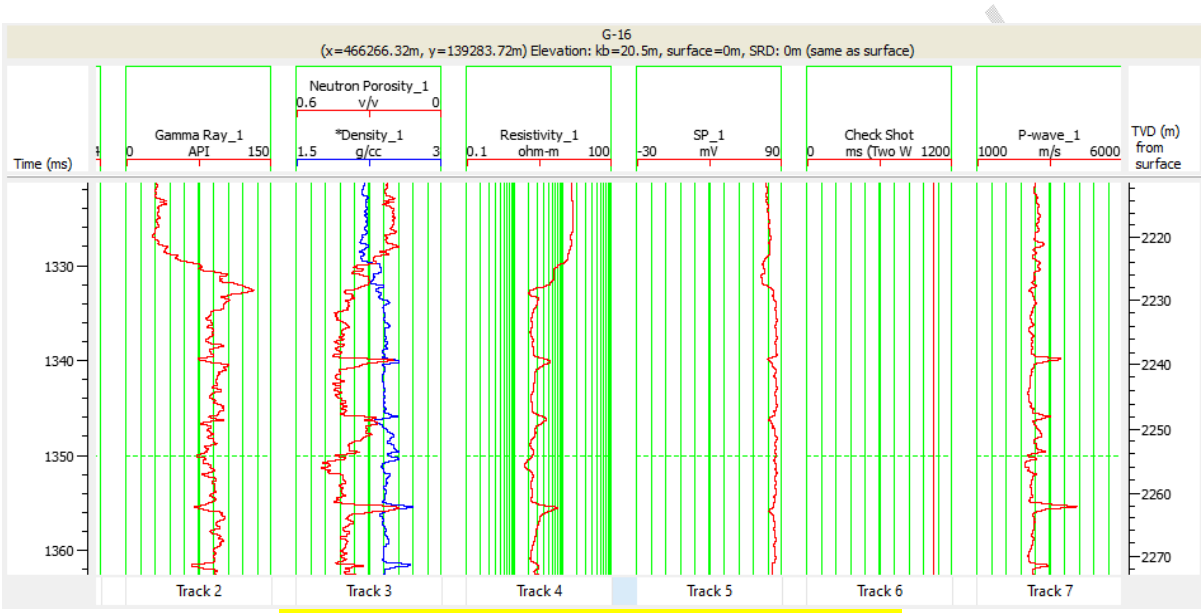

Fig. 7. Typical log section displays of raw log suite for G-16.

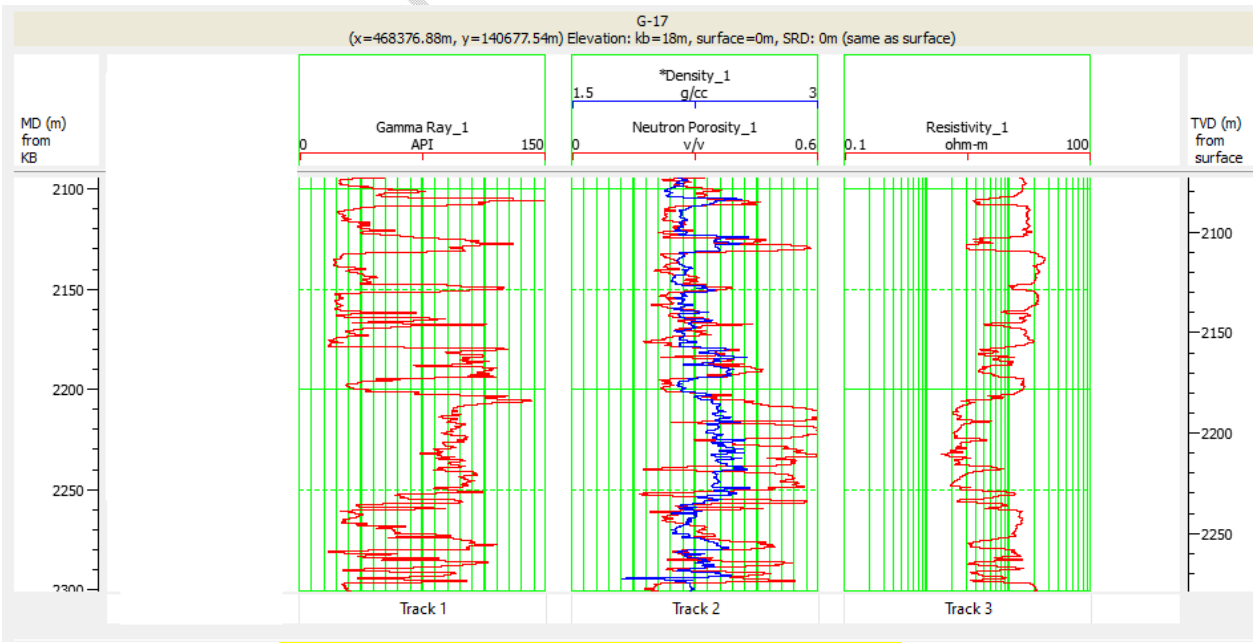

Fig. 8. Typical log section displays of raw log suite for G-17.

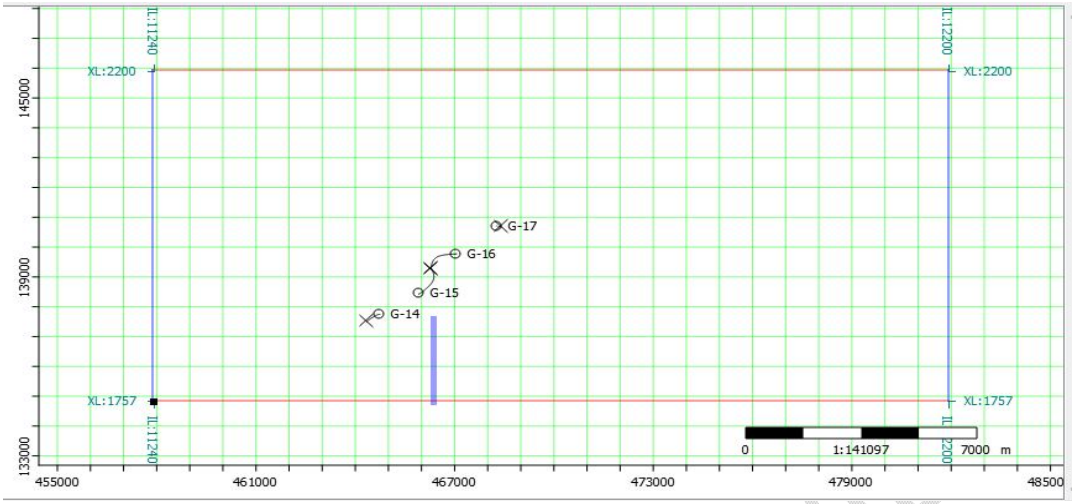

Fig. 9. Base Map of study area.

To achieve the main objective of this study, several processes and techniques were implemented these include:- Quality check, Well log interpretation, Well correlation, AVO modeling and analysis, seismic to well tie, seismic horizon picking, seismic inversion and reservoir evaluation using seismic attributes.

2.1 Quality Control (QC)

The available data were assessed to ascertain their quality and thus their suitability for this study. For the well data, it was observed that all the wells contain the basic logs required for reservoir evaluation except for of G-17 which did not contain the compressional sonic log and checkshot as such it was not used for most of the analysis. The inconsistency in results obtained from seismic data (in time units) and well log data (in depth unit) was balanced using checkshot data. Detailed information of logs available in each log suite for each of the wells is given in Table3. For the seismic data, we observed it was of the same field as the wells, the quality was good and showed the events clearly to allow for reliable mapping and interpretation.

Table 3. Suite of Logs in each Well **(Y=YES, N=NO).**

WELLS	AVAILABLE LOGS							
	GR	RT	RHOB	NPHI	DT	CALI	SP	CS
G-14	Y	Y	Y	Y	Y	Y	Y	Y
G-15	Y	Y	Y	Y	Y	Y	Y	Y
G-16	Y	Y	Y	Y	Y	N	Y	Y
G-17	Y	Y	Y	Y	N	N	N	N

2.2 Well Correlation

Well correlation was carried out in a bid to identify the specific hydrocarbon bearing sands and this was done with the integration of Gamma Ray, Resistivity, Neutron and Density logs. Three hydrocarbon bearing reservoirs were identified and correlated in the four wells (G-14, G-15, G-16 and G-17) (Fig.10).

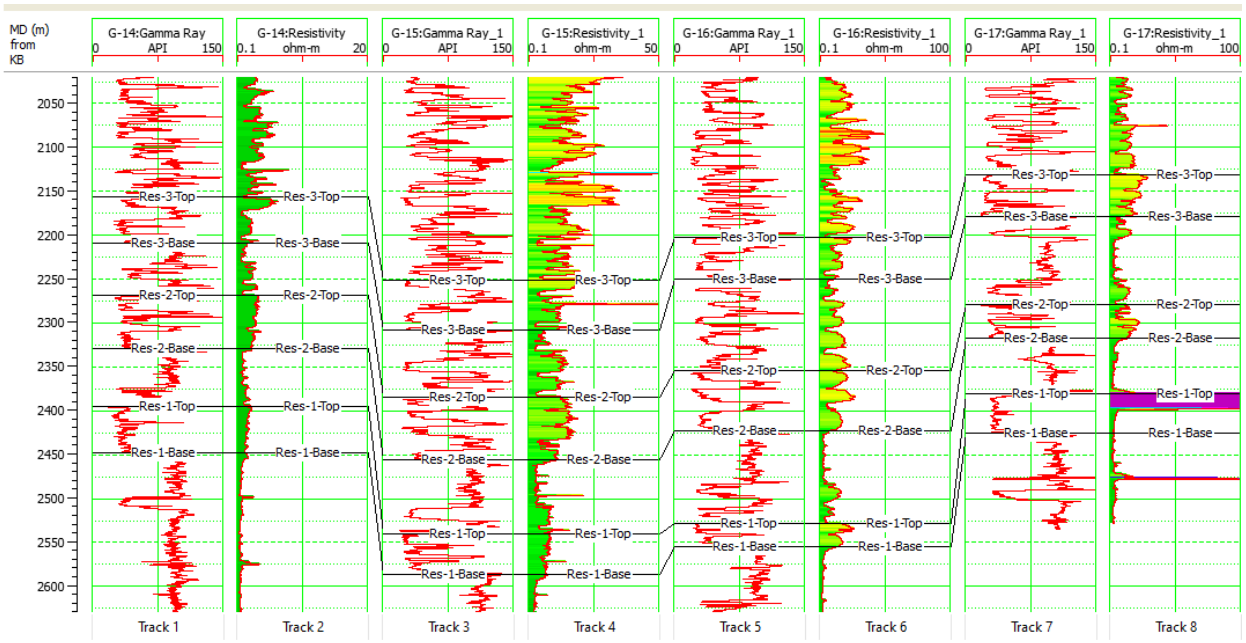

Fig. 10. Well correlation depicting the different lithologies.

2.3 Seismic to Well Tie

To facilitate horizon mapping on the seismic data section, well correlation and seismic to well tie were performed. The seismic data set was then inverted into an impedance volume using a model-based inversion scheme which entails creating a low frequency model guided by well-logs and interpreted horizons. Finally, other elastic attribute properties such as lambda-rho and mu-rho were extracted from the impedance volume along the seismic horizon and used to characterize the reservoir across

2.4 Horizon Interpretation

In our interpretation soft events were interpreted as troughs (blue on the seismic color scheme) while the hard events are interpreted as peaks (red on the seismic color scheme). The interpretation was manually done a one-step increment on every inline and crossline across the seismic for proper accuracy, two horizons were mapped out and guided by reservoir markers in well logs.

2.5 AVO Modeling

Well log data were analyzed to verify, develop and simulate AVO scenes or scenarios to aid AVO analysis. AVO analysis is widely used in hydrocarbon exploration to distinguish between non-hydrocarbon and hydrocarbon hosting rocks [1, 41].

2.6 Seismic Inversion

After extraction of relevant properties from the seismic data, seismic inversion was performed to determine the formation rock properties contained in the raw seismic record.

For this study, two methods of seismic inversion were implemented, which included the model based inversion which involves deriving an initial model from the wells. Using this model and the extracted average wavelet, a synthetic trace is calculated and compared with the actual seismic data to calculate the error or misfit between them (objective function). The model is then modified iteratively to minimize the error until the inversion converges, i.e. a reasonable solution or an acceptable match is obtained [2, 42, 43]. The second method involves the use of neural networks.

3. RESULTS

3.1 Lithostratigraphic Analysis

Gamma-ray was used to delineate lithology (sand and shale bodies). Sand bodies were identified by a deflection to the left owing to the reduced concentration of radioactive elements in the sand, whereas shale was identified by a deflection to the right due to the high concentration of radioactive elements in shale. The resistivity log was used with the Gamma-ray log to delineate potential reservoirs. High resistivity intervals are thought to be hydrocarbon-bearing intervals, whereas low resistivity zones are thought to be water-bearing intervals. Neutron and density logs were used to determine the hydrocarbon type present in the reservoir (oil or gas), both density and neutron logs are paired in a track with one of their curves reversed giving rise to the balloon effect (used to differentiate the hydrocarbon present). Well correlation was performed in order to identify hydrocarbon-bearing sands, and this was accomplished through the integration of Gamma Ray, Resistivity, Neutron, and Density logs. The well logs show three hydrocarbon potential grains of sand whose tops and base are marked. Identified and correlated by formation tops (Fig. 10).

3.2 AVO Analysis

For the fluid-substituted brine, oil, and gas cases, AVO responses were modeled. The seismic response with increasing offset angle was calculated using Aki and Richard's modified Zoeprittz equation [44]. AVO plots for the sands were displayed as models. Figs. 11-12 show that Reservoir 3 sand exhibits a typical class II AVO response in the study area. The AVO has a small negative intercept (normal incidence), followed by larger amplitudes at large offsets. However, there is a small and barely discernible difference between the *in situ*, oil, and brine responses (it was modeled as an isotropic condition). These results imply that the oil and gas would have similar seismic amplitudes and behave similarly in the near and far seismic stacks.

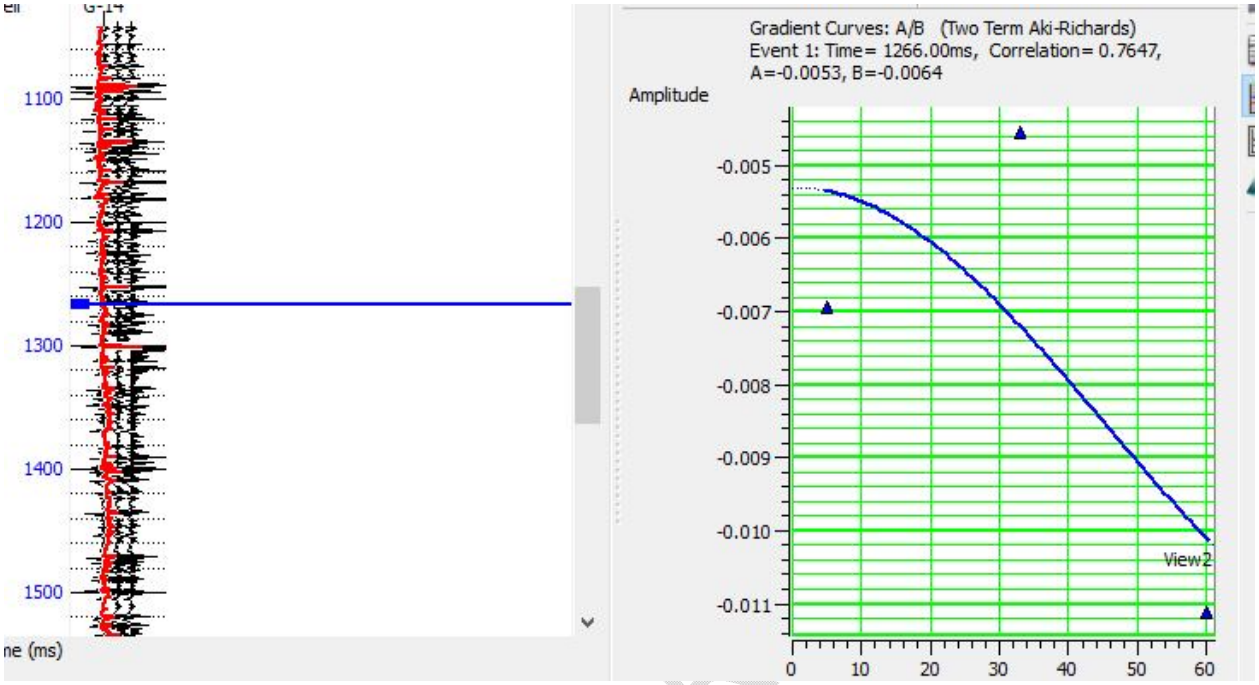

Fig. 11. Class II AVO response of G-14, Reservoir 3 Well top

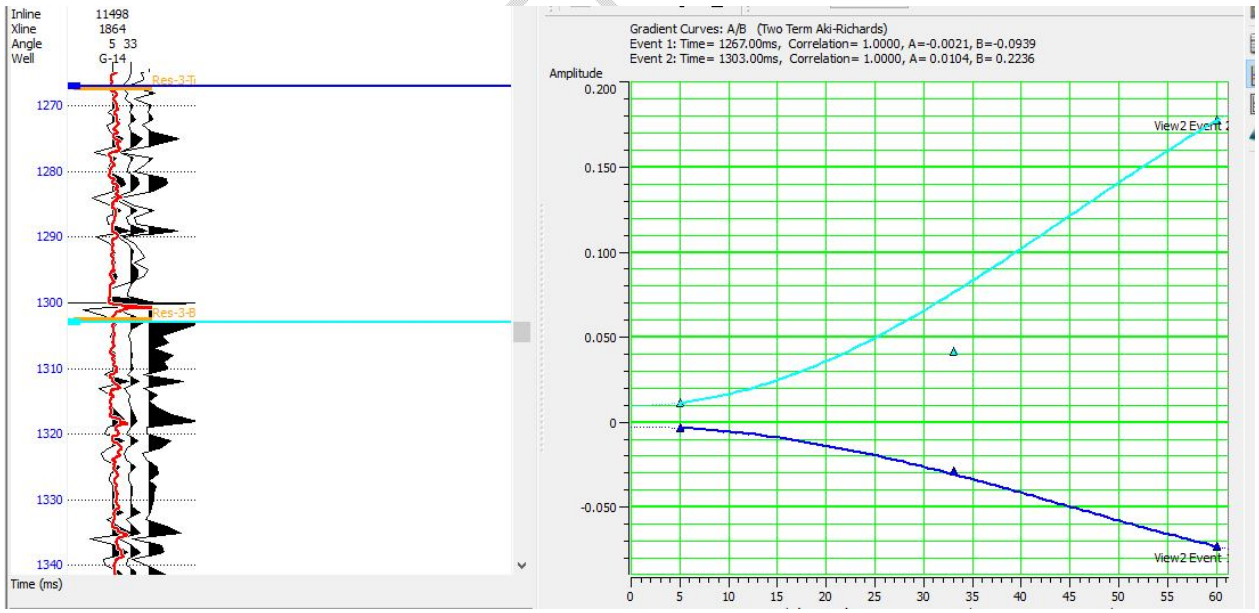

Fig. 12. Class II and Flat spot AVO response of G-14, Reservoir 3 Well top, and base

3.3 Structural Interpretation

The seismic and wells were correlated, and two horizons were chosen and mapped as a result of detailed seismic analysis. They were plotted on the in-lines and cross-lines that ran

through the study area. The geometrical configuration of the stratigraphic surfaces displayed as seismic grids is represented by these mapped surfaces (Figs. 13 – 14).

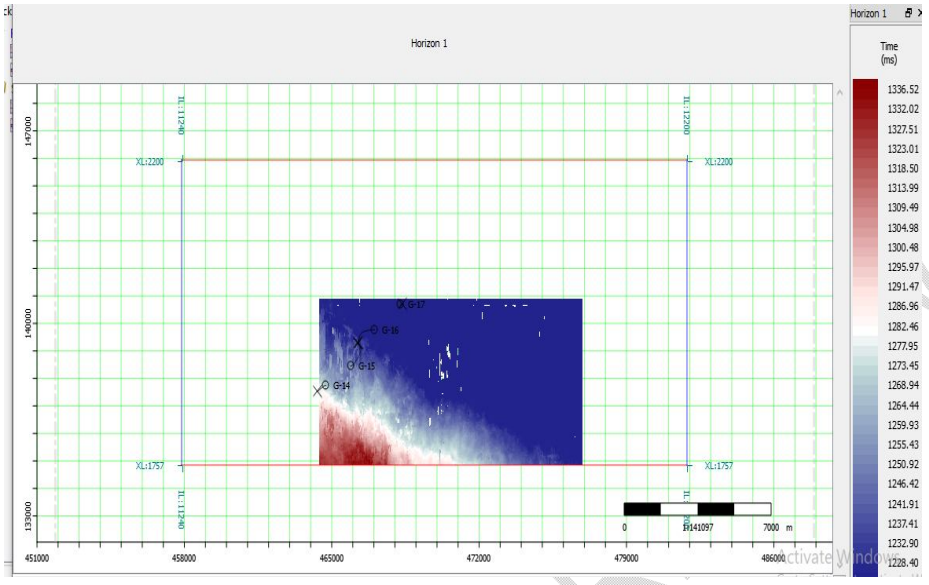

Fig. 13. Mapped result of the first Horizon (Horizon 1) on Inlines and Crosslines.

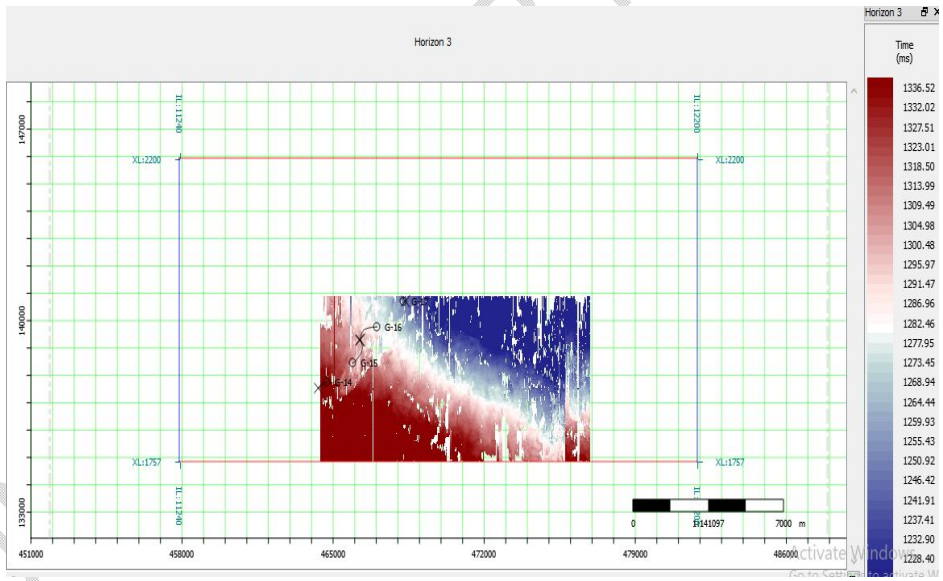

Fig. 14. Mapped result of the second Horizon (Horizon 3) on Inlines and Crosslines.

3.4 Seismic Interpretation

To convert well data into the time domain, check shot data was used. For the processing of a good and reliable horizon interpretation of the data to be performed, a wavelet is extracted to help determine the response expected at the stratigraphic horizons (Figs. 15–17). The reservoir tops conformed to positive amplitudes and are depicted by blue peaks, whereas the reservoir bottoms conform to negative amplitudes and are depicted by red depressions

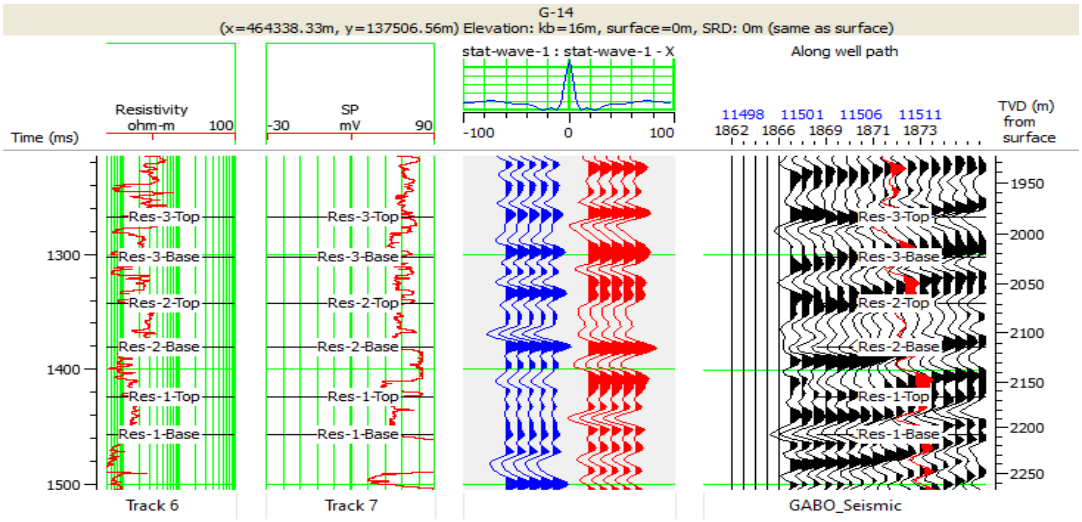

Fig. 15. Seismic well correction for G-14 showing extracted wavelet

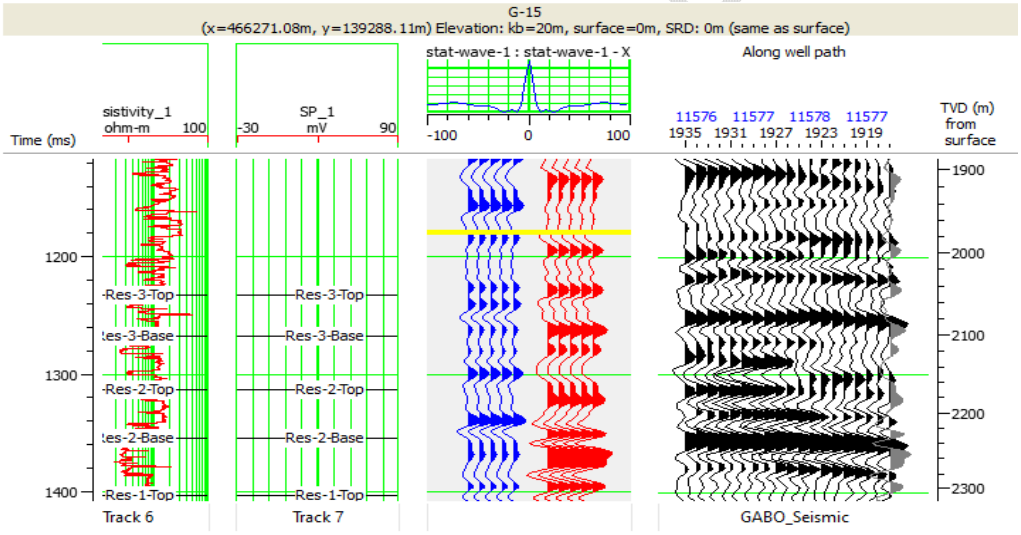

Fig. 16. Seismic well correction for G-15 showing extracted wavelet.

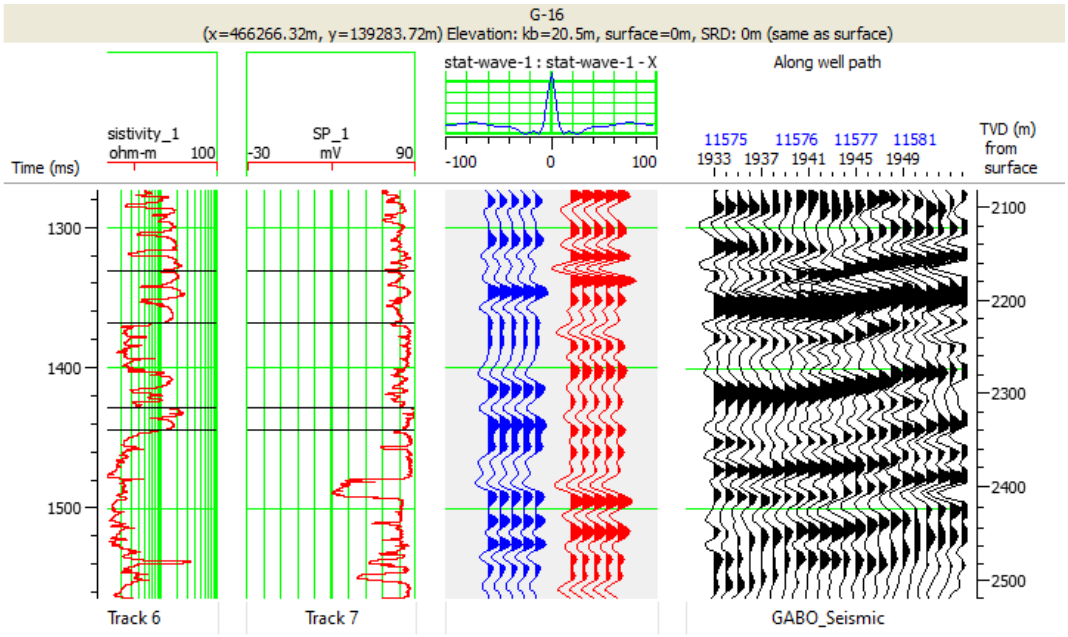

Fig. 17. Seismic well correction for G-16 showing extracted wavelet.

3.5 Seismic Inversion

Using the extracted wavelet both well and seismic data were used to model formations. Two levels of seismic inversion were implemented in this study which involves the procedure of generating an attribute volume of the field using a model-based algorithm and neural networks

3.6 Model Based Inversion

Before modeling, an analysis was performed to see the correlation value between the log of the well data and the log of the inversion results and the fit value between the synthetic seismogram obtained with seismic, the smallest error value is observed to obtain a good correlation between the values from both the inversion results (red) and well data (blue). The correlation is changed iteratively until the difference between the inverted and original traces is less than a certain given value. However, when the synthetic seismogram data with the original seismic data shows a high correlation value, so it can be said to have a very good correlation. With a specific error level close to 0, this means that the results of the pre-inversion parameter settings show good results (Fig. 18). After the correlation a good tie was achieved between the seismic trace and synthetic seismogram Model-based inversion [45] employing a generalized linear inversion algorithm that presumes the seismic trace (S) and wavelet (W) are identified, and later tries to alter the original model until the resulting synthetic matches the seismic trace [46]. This technique works well when there is a good understanding of the geology and a reliable model can be formed. The results of the model based inversion are presented as Acoustic Impedance (Fig. 19), Shear Impedance (Fig. 20), Lambda rho (Fig. 21) and Mu-rho (Fig. 22).

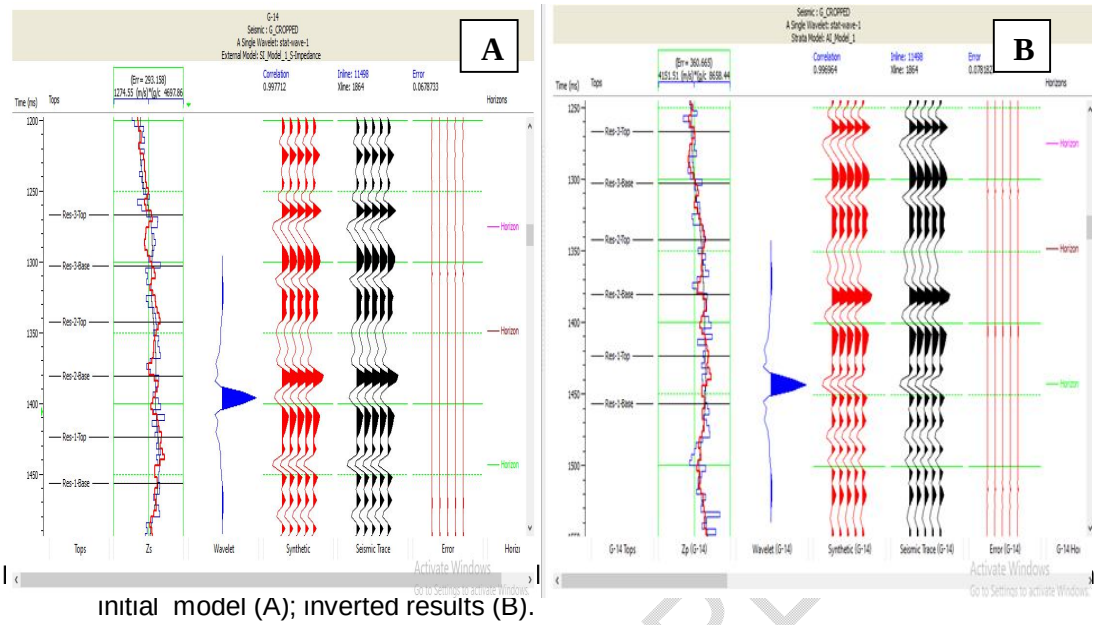

Initial model (A); inverted results (B).

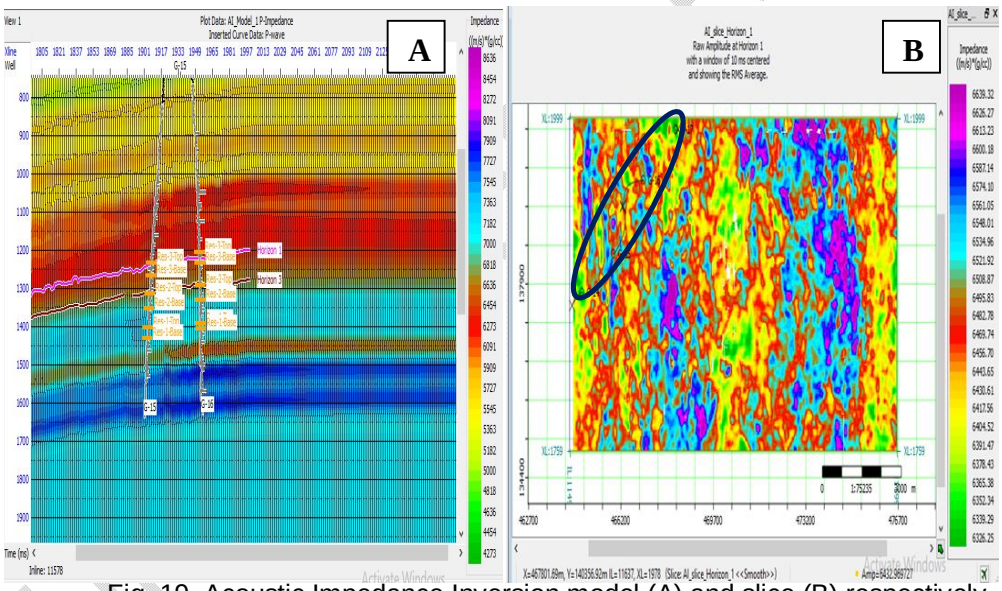

Fig. 19. Acoustic Impedance Inversion model (A) and slice (B) respectively

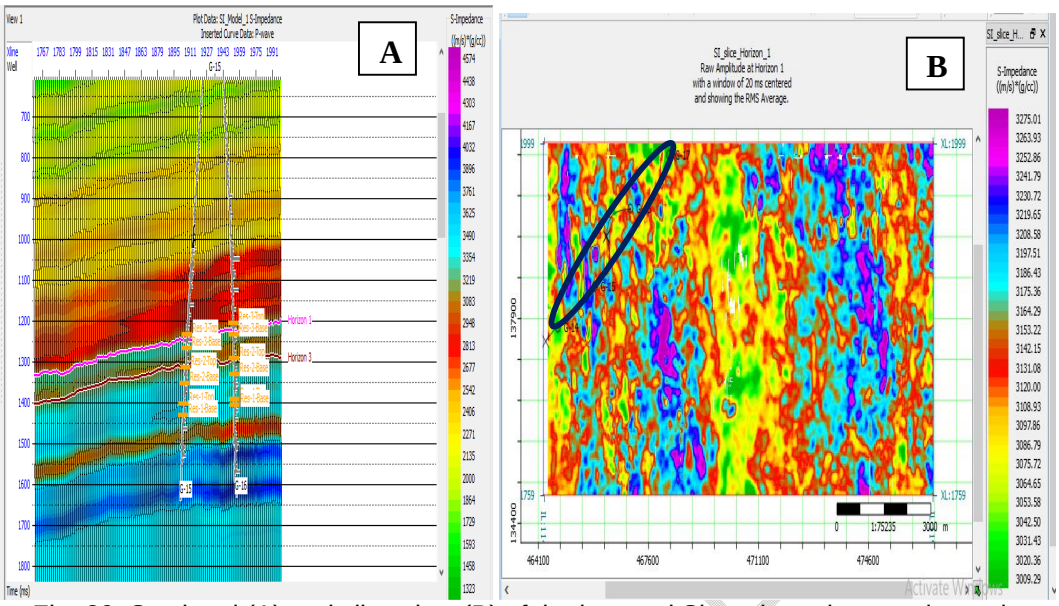

Fig. 20. Sectional (A) and slice view (B) of the inverted Shear impedance volume data.

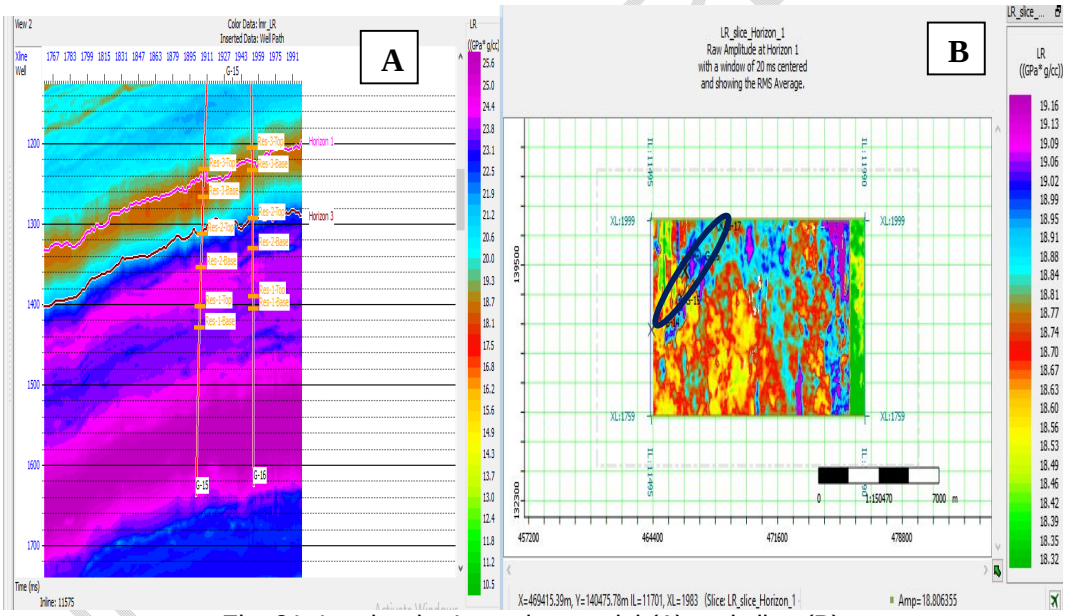

Fig. 21. Lamba rho Inversion model (A) and slice (B)

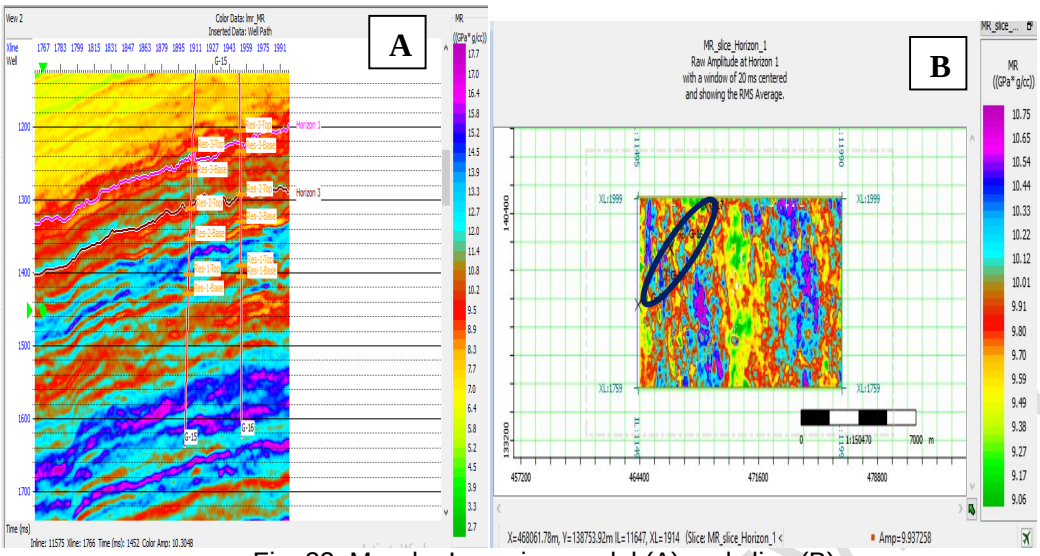

Fig. 22. Mu- rho Inversion model (A) and slice (B)

3.7 Neural Network Inversion

The Emerge module in Hampson Russell software was used for this purpose. A sample set obtained from the well logs was split into training, validation and test subsets. Probabilistic Neural Network (PNN) analysis was then performed on the target log parameter using the seismic volume. The algorithm functions by determining the relationship between the seismic trace and the target reservoir attributes. The training networks were used to observe and learn these relationships from which an estimated target attribute was determined. The target log parameter used for this analysis included: Vp/Vs (Fig. 23), Water saturation (Fig. 24), and Porosity (Fig. 25).

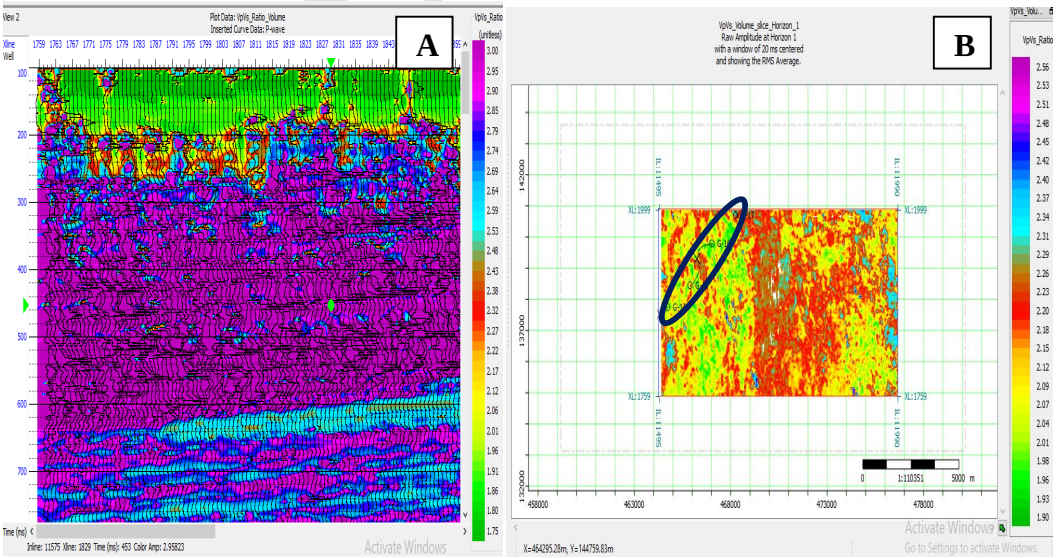

Fig. 23. VP/Vs inverted volume using neural network (A) and slice (B).

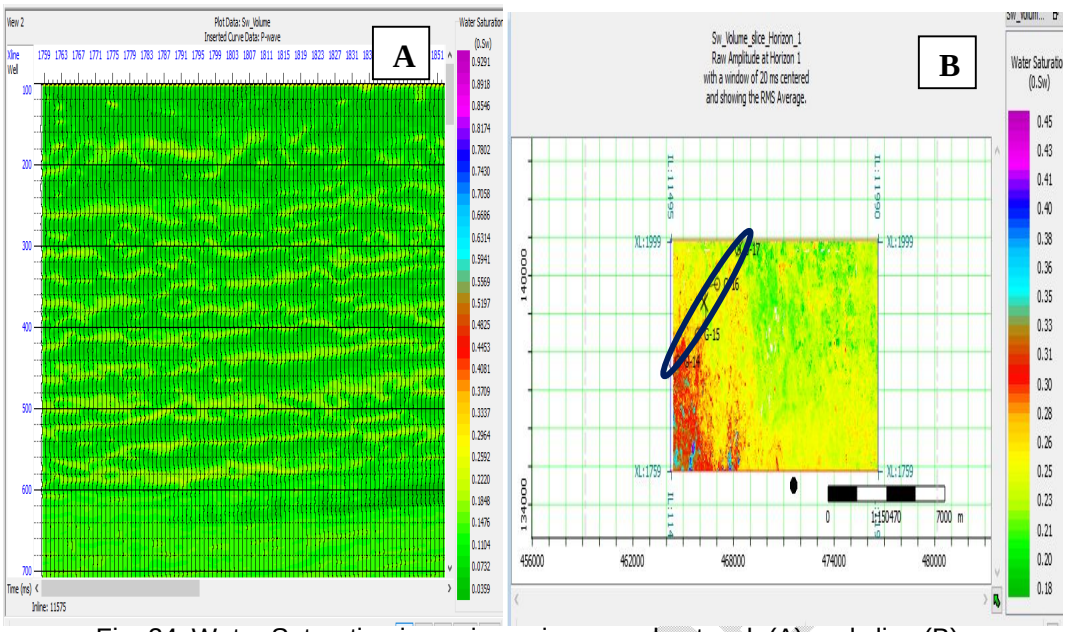

Fig. 24. Water Saturation inversion using neural network (A) and slice (B).

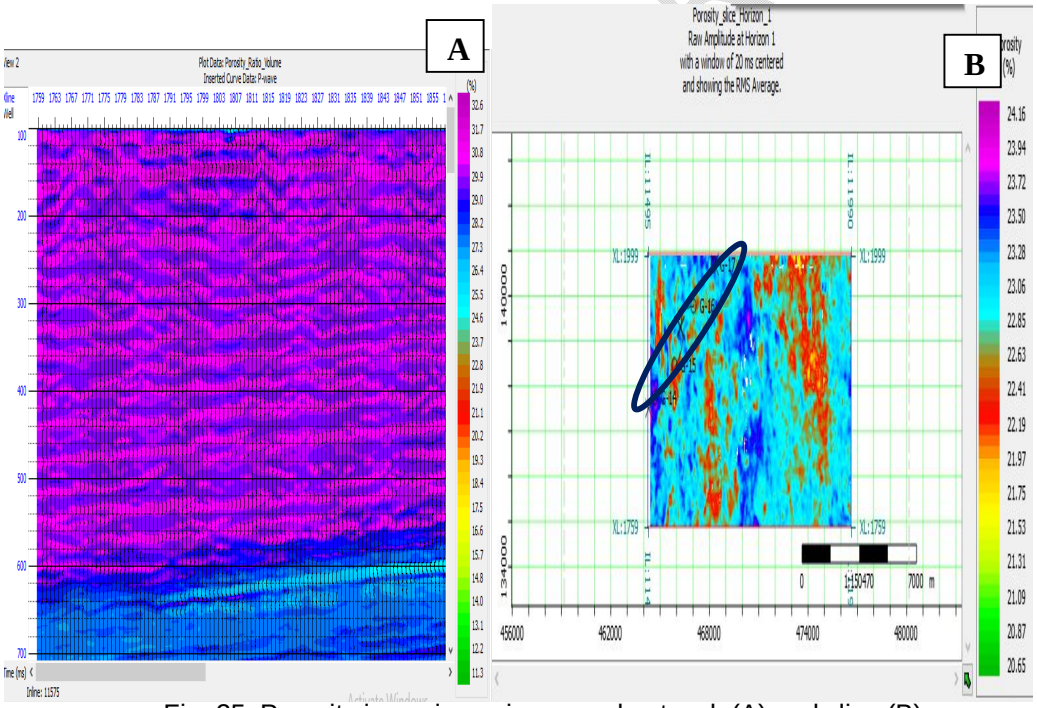

Fig. 25. Porosity inversion using neural network (A) and slice (B).

4. DISCUSSION

Fig. 10 shows well log correlation connecting all four (4) wells within the study area. Reservoir 1, 2 and 3 were identified across all four wells. The gradient analysis performed on the well data revealed that the AVO curves had a small negative intercept with resulting

higher amplitude at far offsets. According to the [12] classification of AVO anomalies shown in Figs. 11–12, the AVO anomaly can be classified as a class II AVO anomaly.

There was a good tie because a check shot correction had been previously performed to get the well to match the seismic data as closely as possible to achieve a proper well to seismic tie. Synthetic seismogram and seismic data correlation for the three wells are shown in Figs. 15–17, because of the unavailability of G-17 check shot there was no generated synthetic seismogram done. Two horizons were identified and mapped along each inline and crossline with a one-step increment. Figs.13–14 shows the generated horizon model.
Seismic inversion was then carried on the data using Reservoir 3 sand. Two levels of seismic inversion was employed for this study which include the model based inversion and neural network inversion.

4.1 Model Based Inversion
4.1.1 Acoustic Impedance

The inverted acoustic impedance volume at G-15 and G-16 is shows a consistent increase in acoustic impedance values with increasing depth (Fig. 19A). The colors within the models show variation of P-impedance values ranging from 4273-8636 Pa-s/m^3 which suggest different lithologies within the reservoir. This is consistent with previous research on the porosity-depth trends of sand and shale [47], which established shale as having a parabolic form (relatively declining in acoustic impedance with increased depth) and sands as having a consistent pattern (impedance gradually increasing with depth). Acoustic impedance slice across horizon 1 (Fig. 19B) shows high impedance values around the vicinity of the wells but not in the well location (having a green color code) which is consistent with fluid determination. Low acoustic impedance is an indication of fluid saturated sands (hydrocarbons) (location of drilled wells). Hydrocarbon bearing intervals are characterized by low acoustic impedance and are characteristics of sandstone reservoirs within Agbada formation in Niger Delta [48].

4.1.2 Shear Impedance

The inverted shear impedance volume at G-15 and 16 is shown in Fig. 20A. An increase in shear impedance values with increase in depth. The various colors in the models shows variation of S-impedance altitude ranging from 1323-4574 Pa-s/m^3 which suggest different lithologies within the reservoir model. When compared to the acoustic impedance cross section, the Fig, 20A depicts a much lower impedance value, which corresponds to the findings of [49]. In Fig. 20B, the shear impedance slice across horizon 1 shows high impedance to lower impedance value variations is observed around the surrounding areas of the wells. However, the well location has a generally low impedance value which is consistent with fluid determination using inversion being that low shear impedance is an indication of fluid saturated sands (hydrocarbons) which coincided with the position where the wells are drilled.

4.1.3 Lambda–Rho

Lambda–Rho volume, which is a physical change in the pore space when subjected to pressure, can be used to predict pore fluid content. Changes in rock pores and fluid are more likely to cause this change than changes in grain size. In oil saturated sandstones, incompressibility is low, so Lambda–Rho can be used as an oil/gas content indicator in the pore space. In Fig. 21A, the area surrounding horizon 1 has a low distribution of Lambda–Rho values, which in a sand stone reservoir is the pore fluid equivalent. On the basis of the interpretation and analysis, it is possible to conclude that the reservoir is suitable for oil

accumulation. The Lambda–Rho slice along the horizon (Fig.21B) shows the areas with high prospects for exploration, the locations of each well shows low Lambda–Rho value [50]

4.1.4 Mu–Rho

Mu–Rho (μρ) gives information regarding rock matrix. Fig. 22A show that the area around the horizons picked has a distribution of both medium - high values of Mu-rho, which shows rigidity in the area as is commonly associated with sand-shaly areas. High values of Mu-rho are usually associated with hydrocarbon sand. The Mu–Rho (μρ) horizon slice (Fig. 22B) exhibits high μρ values around the producing well locations with exception of G–17 which might suggest minor shale intrusions or unconsolidated reservoir sands [50].

4.2 Neural Network Inversion

4.2.1 V_P/V_S Inversion

The seismic section's lithology and facies are demarcated by V_P/V_S. It showed a strong relationship with the lithological composition and pore pressure in sub surface rocks [51, 52, 53]. It was also directly related to Poison's ratio and it shows high porous fluids sensitivity [53] and is widely used for potential reservoirs, as an effective hydrocarbon discriminator [54] High Vp/Vs values are noted in the inverted volume of the seismic data (Fig. 23A) indicating a high level of shaly lithology around the study area, also having a variation between a far lower and medium value at the top and also in between. This shaly lithology indicates the presence of sand and brine. The inverted slice (Fig. 23B) shows that all four wells are located in areas with low V_P/V_S values, conceivably indicating the presence of hydrocarbon.

4.2.2 Water Saturation

Low water saturation values were noted in the inverted volume of our seismic data (Fig. 24A) ranging between 0.00399-0.3337, showing a variation with the green and yellow color code. Therefore the water in the reservoir can be said be at a range of about 30- 34% indicating an excellent reservoir. The inverted slice (Fig. 24B) showed how all four wells were in areas with very low water saturation values, probably indicating the presence of hydrocarbon.

4.2.3 Porosity

High porosity values were noted in the inverted volume of our seismic data (Fig. 25A) ranging between 27.3 and 32.6, showing a variation with the purple and blue color-code indicating large pore space for hydrocarbons. However, the inverted slice (Fig. 25B) shows that all four wells are located in areas with very high porosity values, possibly indicating the presence of hydrocarbon.

5. CONCLUSION

This study investigated and characterized reservoir properties via AVO analysis and seismic inversion methods using four conventional well logs acquired in G–field of Niger Delta.

AVO modeling results using well logs proved that changes in amplitude with offset was slightly similar for brine and oil cases. G-14 location was used in AVO analysis, and the result showed a small negative intercept with subsequently higher amplitudes as offset increases for the top demonstrating that Class II anomaly which is known as "phase or polarity reversals", was detected. The base of the reservoir demonstrated a flat spot structure anomaly.

The inversion result also conforms to the structures which makes it a very robust reservoir (having a low water saturation and high porosity value) for hydrocarbon bearing and aided the interpretation of the G–field revealing better reservoir architecture for the field characterization.

Combining all these analyses provided a reliable way to interpret and characterize a reservoir was achieved. From this research, it can be concluded that G–field is an oil field and AVO analysis and seismic inversion is a good seismic interpreter for reservoir characterization.

REFERENCES

Hilterman F. Seismic amplitude interpretation, SEG/EAGE 2001 distinguished instructor short course No. 4: Society of Exploration Geophysicists. 2001.

Sen MK. Seismic inversion, Society of Petroleum Engineers, U.S.A. 2006;120.

Adelu AO, Aderemi AA, Akanji AO, Sanuade OA, Kaka SI, Afolabia O, Olugbemiga S, Oke R. Application of 3D static modeling for optimal reservoir characterization. Journal of African Earth Sciences. 2019;152:184–196

Chopra S, Michelena RJ. Introduction to this special section: reservoir characterization. Lead Edge. 2011;30(1): 35-37

Russell B. Strata workshop: theory and exercises in seismic inversion and AVO (unpublished lecture notes). 2005.

Latimer R. "Uses, abuses, and examples of seismic-derived acoustic impedance data: what does the interpreter need to know?" AAPG Bulletin. 2006; 90.

Singh S, Gupta D, Rajput S. Pre-stack seismic inversion and amplitude versus angle modeling reduces the risk in hydrocarbon prospect evaluation. Advances in Petroleum Exploration and Development. 2014;7(2):30-39.

Feng H, Bancroft JC.AVO principles, processing and inversion CREWES Research Report 18. 2006

Ostrander WJ. Plane-wave reflection coefficients for gas sands at non-normal angles of incidence: Geophysics. 1984;49(10):1637–1648.

Castagna JP, Swan HW. Principles of AVO cross-plotting. The Leading Edge. 1997;16(4): 337-342.

Castagna JP, Swan HW, Foster DJ. Framework for AVO gradient and intercept interpretation: Geophysics. 1998;63(3):984-956.

Rutherford SR, Williams RH. Amplitude-versus-offset variations in gas sands: Geophysics, 1989;54(6):680–688.

Wang Y, Houseman GA. Tomographic inversion of reflection seismic amplitude data for velocity variation. Geophys. J. Internat.1995;123(2):355–372.

Wang Y, Pratt RG. Sensitivities of seismic traveltimes and amplitudes in reflection tomography: Geophys. J. Internat. 1997;131(4):618–642.

Surender S, Gupta DK, Sanjeev R. Pre-stack seismic inversion and amplitude versus angle modeling reduces the risk in hydrocarbon prospect evaluation. Advances in Petroleum Exploration and Development. 2014;7(2):30-39.

Ogagarue DO, Anine LA. An integration of rock physics, AVO modeling and analysis for reservoir fluid and lithology discrimination in a Niger Delta deepwater block. IOSR J. Appl. Geol. Geophys. 2016;4(2):36-46.

Vernengo L, Trinchero E, Chopra S. Deciphering seismic amplitude language. American Association of Petroleum Geologist Explorer Geophysical. Corner. 2017;20–21

Ogbamikhumi A, Igbinigie NS. Rock physics attribute analysis for hydrocarbon prospectivity in the Eva field onshore Niger Delta Basin. J. Pet. Explor. Prod. Technol. 2020;10:3127–3138

Allo OJ, Ayolabi EA, Adeoti L, Akinmosin A, Oladele S. Reservoir characterization for hydrocarbon detection using Amplitude Variation with Angles constrained by localized rock physics template Journal of African Earth Sciences 2022;192: 104548

Adeoti LA, Olawale A, Elijah A, Adewale A, Oladele S, Taiwo A. Ayuk MA. Reservoir fluid determination from angle stacked seismic volumes in 'Jay' Field, Niger Delta, Nigeria. J. Appl. Sci. Environ. Manage. 2018;22(4):453–458

Ajanaku BS,Akintorinwa OJ. Determination of gas reservoir(s) using AVO inversion within "XY" field offshore Niger Delta. Petroleum Research. 2019;4(1):52-58.

Avseth P, Lehocki I. Combining burial history and rock-physics modeling to constrain AVO analysis during exploration. Lead. Edge. 2016:35:936–945

Ridwan TK, Hermana M, Lubis LA, Riyadi ZA. New AVO attributes and their applications for facies and hydrocarbon prediction: a case study from the northern Malay basin. Appl. Sci. 2020;10:7786–7803.

Hussein M, Abu El-Ata A, El-Behiry M. AVO analysis aids in differentiation between false and true amplitude responses: a case study of El Mansoura field, onshore Nile Delta, Egypt. J. Pet. Explor. Prod. Technol. 2020;10:969–989.

Hu Q, Innanen K. Rock physics properties from seismic attributes with global optimization methods. CREWES, Geoconvention, September. Canada. 2021;13–15.

Ogbamikhumi A, Omorogieva OM. Rock property modelling and sensitivity analysis for hydrocarbon exploration in OSSY Field, Niger Delta Basin. J. Pet. Explor. Prod. Technol. 2021:11:1809–1822.

Agbasi O, Sen S, Inyang N, Etuk S. Assessment of pore pressure, wellbore failure and reservoir stability in the Gabo field, Niger Delta, Nigeria - Implications for drilling and reservoir management. Journal of African Earth Sciences. 2020;173;104038.

Turtle MLW, Charpentier RR, Brownfield ME. The Niger Delta petroleum system: Niger Delta Province, Nigeria, Cameroun, and Equatorial Guinea, Africa. U.S.G.S. Open file Report. 1999;50–54.

Adeoti L. Adeleye KO, Itsemode A, Bello MA. Fluid prediction using AVO analysis and forward modelling of deep reservoirs in Faith Field, Niger Delta, Nigeria. Arabian Journal of Geosciences. 2014;8(6):4057–4074.

Klett TR, Ahlbrandt TS, Schmoker JW, Dolton JL. Ranking of the world's oil and gas provinces by known petroleum volumes: U.S. Geological Survey Open-file Report-1997;97-463.

Whiteman AJ. Nigeria: its petroleum geology, resources and potential I & II. Graham and Trotman, Edinburgh. 1982

Doust H, Omatsola E. Niger Delta. In: Edwards JD, Santogrossi PA (eds) Divergent and passive basins. AAPG, Tulsa, Memoir. 1990;48:239–248.

Kulke H. Nigeria. In: Kulke H (ed) Regional petroleum geology of the world. part II: Africa America, Australia and Antarctica. Gebruder Borntraeger, Berlin. 1995;6(2): 143–172.

Kaplan A, Lusser CV, Norton IO. Tectonic map of the world. panel 10 Tulsa. AAPG Bull. 1994;74:1–1

Hospers J. Gravity field and structure of Niger Delta, Nigeria. West Afr Bull GeolSoc Am. 1965;76(6):407–422.

Feng H, Bancroft, JC. AVO principles, processing and inversion CREWES Research Report 18. 2006.

Veeken P, Rauch-Davies M. AVO attribute analysis and seismic reservoir characterization. EAGE. First Break. 2006;24:41-52 KMS Technologies KJT Enterprises Inc. Publication.
Avseth P, Mukerji T, Mavko G. Quantitative seismic interpretation: applying rock physics tools to reduce interpretation risk. Cambridge University Press. 2005;13(1):545-560
Rutherford SR. and Williams RH. Amplitude-versus-offset variations in gas sands Geophysics. 1989;54(6):680-688
Ross CP, Kinman DL. Nonbright-spot AVO: Two examples: Geophysics.1995;60(5):1398-1408
Jing-Ye L. Gas reservoir identification by seismic AVO attributes on fluid substitution. ApplGeophys. 2012;9:139–148.
Russell, B. Strata Workshop: theory and exercises in seismic inversion and AVO (unpublished lecture notes). 2005
Shrestha RK. Reservoir characterization of high impedance sands in the Ada field, North Louisiana, USA: GSH/SEG Spring Symposium Technical Program, 5. 2008.
Aki K, Richards P. Quantitative seismology—theory and methods. W. H. Freeman &Co. 1980;16(1):726-728.
Russell B, Hampson D. Comparison of poststack inversion methods: 61St Annual International Meeting, SEG, Expanded Abstracts 1991;10:876-878.
Cooke DA, Schneider WA. Generalized linear inversion of reflection seismic data: Geophysics, 1983;48(6):665-676.
Olowokere MT, Ojo JS. Porosity and lithology prediction in Eve Field, Niger Delta using compaction curves and rock physics. International Journal of Geosciences. 2011;2(3):366-372.
Tamuko O.J. 3D Seismic structural interpretation and petrophysical evaluation of X-field, Niger Delta Basin, Nigeria, B.Tech Unpublished Project, Federal University of Technology Akure (FUTA). 2008.
Akpan AS, Okeke FN, Obiora DN, George NJ. Modelling and mapping hydrocarbon saturated sand reservoir using Poisson's impedance (PI) inversion: a case study of Bonna field, Niger Delta swamp depobelt, Nigeria."Journal of Petroleum Exploration and Production Technology. 2021;11(1):117-132.
Dagogo T, Ehirim CN, Ebeniro JO. Enhanced prospect definition using well and 4D seismic data in a Niger Delta Field. International Journal of Geosciences. 2016;7(8):977-990.
Wilkens R, Simmons G, Caruso L. The ratio Vp/Vs as a discriminant of composition for siliceous limestones. Geophysics. 1984;49(11):1850-1860.
Zimmer M, Prasad M, Mavko G. Pressure and porosity influences on Vp/Vs ratio in unconsolidated impedance inversion. Geophysical Prospecting. 2002;55(6):819-833.
Wang X, Schubnel A, Fortin J, David EC, Gueguen Y, Ge H. High Vp/Vs ratio: saturated cracks or anisotropy effects. Geophysical Research Letters. 2012;39(11):11307.
Hamanada GM. Reservoir fluid identification using Vp/Vs ratio. Oil and Gas Science Technology. 2004;59(6):649-654.